X-ray tomography to measure size of fragments from penetration of high-velocity tungsten rods

Zach Stone, Stephan Bless, John Tolman, Jason McDonald, Scott Levinson, and R. Hanna

Articles you may be interested in

A computational study of segmented tungsten rod penetration into a thick steel target plate at high velocities
AIP Conf. Proc. **1426**, 80 (2012); 10.1063/1.3686226

Modelling the X-ray spectra of high-velocity outflows from quasars
AIP Conf. Proc. **774**, 369 (2005); 10.1063/1.1960955

Grating X-ray Spectroscopy of High-Velocity Outflows from Active Galaxies
AIP Conf. Proc. **645**, 119 (2002); 10.1063/1.1525444

Target strength of ceramic materials for high-velocity penetration
J. Appl. Phys. **67**, 3669 (1990); 10.1063/1.345322

Analysis of High-Velocity Projectile Penetration Mechanics
J. Appl. Phys. **37**, 1579 (1966); 10.1063/1.1708570

X-RAY TOMOGRAPHY TO MEASURE SIZE OF FRAGMENTS FROM PENETRATION OF HIGH-VELOCITY TUNGSTEN RODS

Z. Stone[1], S. Bless[1], J. Tolman[1], J. McDonald[1], S. Levinson[1], and R. Hanna[2]

[1]*Institute for Advanced Technology, The University of Texas at Austin*
[2]*Jackson School, The University of Texas at Austin*

Abstract. Behind-armor debris that results from tungsten rods penetrating armor steel at 2 km/s was studied by analysis of recovered fragments. Fragment recovery was by means of particle board. Individual fragments were analyzed by x-ray tomography, which provides information for fragment identification, mass, shape, and penetration down to masses of a few milligrams. The experiments were complemented by AUTODYN and EPIC calculations. Fragments were steel or tungsten generated from the channel or from the breakout through the target rear surface. Channel fragment motions were well described by Tate theory. Breakout fragments had velocities from the projectile remnant to the channel velocity, apparently depending on where in the projectile a fragment originated. The fragment size distribution was extremely broad and did not correlate well with simple uniform-fragment-size models.

Keywords: Fragmentation, Terminal Ballistics.
PACS: 46.50.+a, 45.40.G

INTRODUCTION

The effectiveness of anti-armor penetrators can be measured in two ways. The first and simplest is penetration. The most common measure of penetration is that normalized by the cube root of impact kinetic energy $P/(KE)^{1/3}$. This parameter is called *penetrator efficiency*. It is equivalent to the penetration per unit of kinetic energy. The normalization is by the cube root of the energy in order to achieve a metric that is scale independent (at least to the extent that penetration is proportional to length). Thus, this parameter provides a framework for evaluating the effect of velocity as well as shape. It has been used, for example, to compare penetrator designs across a range of velocities and targets. This measure of effectiveness is especially useful when penetrators at a common kinetic energy (CKE) are compared.

However, in weapon-system design, there is a requirement for penetrators to achieve a specified *lethality*. Lethality is measured as $P_{K/H}$, the probability of kill given a hit on a target vehicle. The lethality of a given penetrator is both target and scenario dependent. Determination of lethality for a given target/penetrator combination requires a great number of experiments and data analysis, as described, for example, in [1].

Lethality depends primarily on behind-armor debris (BAD)—the particles that are projected behind the target. BAD particles come from the projectile and the target and are generated during the breakout or exit stage of penetration, in which the target material in front of the projectile fails. The appearance of an armor steel target that has been perforated by a high velocity tungsten alloy rod is shown in Fig. 1.

According to what is conventionally called the Tate model, after [2], when a rod projectile strikes

a target at velocity v and penetrates at velocity u, then the velocity of the eroded debris of the penetrator is $2u - v$. Note that u can be computed from g = penetration/length, as $gv/(1 + g)$. The average strain rate for material that erodes from the penetrator is of the order of the consumption velocity divided by rod diameter $(v - u)/D$. For material that is in a homogeneous tensile strain field, in which the expansion energy is available to create new surface area, Grady [3] has shown that the distance between failures (interpreted to be the average particle size) is proportional to strain rate to the $-2/3$ power. The volume of the rod available to form fragments during projectile exit is probably proportional to D^3, and one would expect that the number of fragments is proportional to D/s. If the Grady model is correct, then one would expect that for constant velocity, the number of fragments should be proportional to $D^{1/3}$. For CKE projectiles, D varies as $V^{2/3}$, and the number of fragments would vary approximately as $V^{4/9}$. We refer to this as the IAT model for number of fragments as a function of velocity.
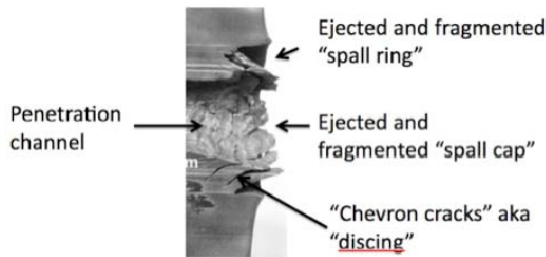

Figure 1. Appearance of target exit.

When tungsten rods penetrate aluminum, all of the fragments of interest are from the penetrator. For that case, it has been shown that the IAT model qualitatively accounts for the dependence of the number of fragments on penetrator diameter and velocity [4].

The geometric form of particle fields behind the target is usually treated in the framework proposed by Mayseless [5] and Saucier [1]. Both the target and projectile fragments are presumed to have similar velocities and to lie on the surface of an expanding and propagating truncated ellipsoid.

EXPERIMENTS

L/D=20 rods 6.35 mm diameter made from 91% W-Ni=Co alloy were fired at nominally 2 km/s at 76 mm thick armor steel targets.

This work took a new approach to characterize BAD based on x-ray tomography. The scanning was performed by the high-resolution x-ray computed tomography (XCT) facility at the University of Texas at Austin Department of Geological Sciences. This is a national shared multi-user facility supported by the National Science Foundation (NSF) Earth Sciences Directorate [6]. Analysis of XCT data was accomplished with a program written at the University of Texas—BLOB. This program was designed to measure three-dimensional geometric information up to thousands of discrete objects, such as behind-armor debris, within a CT data volume. The resolution obtained with these procedures for particle detection was 1 voxel = 0.021 mm^3.

A medium was required that would have a reasonable depth of penetration: all particles should penetrate, but penetrations of more than a few inches would create unnecessary expense in the XCT process. Extensive data for Celotex [7] and wallboard [8] were examined. It was decided to use a more consolidated epoxy-cellulose product, medium density fiberboard (MDF). The density of this material was 0.6 g/cm^3.

In the design of the placement of MDF behind the target, it was decided to avoid possible obliquity effects by deploying the MDF in a circular arc centered on the exit point of the target. This arrangement also had the advantage that, except for a very slight lateral correction, the solid angle subtended by the MDF was not a function of departure angle. The distance from the exit point on the target to the MDF was 508 mm (20 inches). The width of the MDF was 200 mm. The geometry of the MDF deployment is sketched in Fig. 2. The MDF arcs were held in place by aluminum clamps and through-bolts. X-rays of the BAD pattern were also obtained with multiple exposures.

Radiography was also employed behind the target. Considering the various tradeoffs in placement of x-ray cassettes, it was decided to place the cassettes relatively close to the shot line, so that even small particles could be imaged. The

magnification achieved with this setup was only 1.1. However, in order to protect the x-ray cassettes from direct impact and damage, it was necessary to shield them from the fragment spray by putting a steel plate behind the target just off the shot line. Six x-ray plates were exposed simultaneously. All fragments at less than about 45 degrees' departure angle were probably captured in the films. The total field of view was such that when the x-rays were triggered to capture the fastest particle at the far edge of the field of view, all particles with speeds between about 400 and 2000 m/s were imaged.

RESULTS OF EXPERIMENTS AND MODELING

Targets were sectioned, and it was found that entrance-hole diameters were approximately 10.6 mm. Exit holes were approximately 16 mm in diameter. In the center, the diameter was about 15.5 mm. Hence, the ratio of hole diameter to projectile diameter was 2.8 at 2 km/s. This was larger than the value predicted by the Silsby formula [9], which was 2.3. All targets exhibited a spall ring. However, only in half the shots did the spall ring detach.

The x-rays captured an image of the residual rod penetrator, as shown in Fig. 3. It turned out that the target thickness divided by the eroded length of the rod was slightly more than the penetration normalized by length for shots into semi-infinite targets [10]. It thus appears that excess erosion after target exit (see, e.g. [11]) is more important than the "softening" associated with approach to a free surface.

Contrary to the debris bubble model, there are a small number of particles in the 10 to 100 mg range that are lined up behind the penetrator. The velocity of these fastest fragments is only about 10% lower than the residual penetrator velocity.

Analysis of radiographs found a virtually uncountable number of slow fragments, evidently the channel fragments predicted by Tate analysis. In particular there was a dense cloud of particles on axis that had velocities of several hundred meters per second. Relative fragment masses were computed from the area of fragment images raised to the 2/3 power. A correction factor was applied based on calibration radiographs. There was no correlation between particle velocity (e.g., position) and mass.
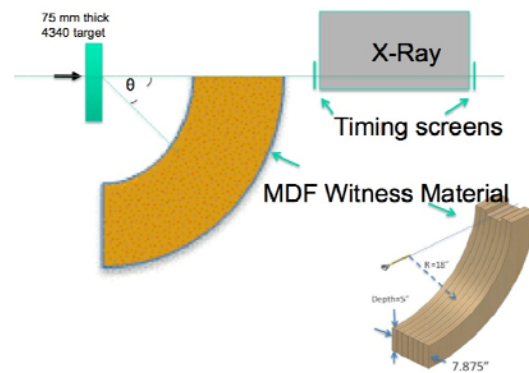

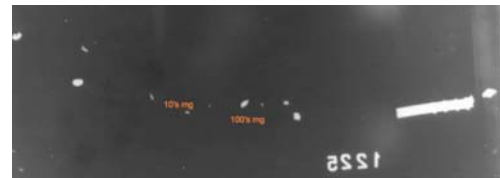**Figure 2.** MDF placement with respect to target.

Figure 3. An example of the fastest fragments.

Particles caught in MDF were analyzed with XCT. Fragment flux was computed as the number of fragments per unit solid angle. Results are shown in Fig. 4 for two experiments. In these figures, the data for angles less than 4 degrees are unreliable because of erosion of the particleboard caused by the high density of impacts close to the shot line. Both shots show a decline from the near-shot-line peak beyond about 4 degrees, to a level of about 20 particles per steradian. There may be a local maximum at about 10 degrees. The flux at larger angles was a little higher in shot 1225 than in shot 1224.

To summarize the experimental findings: the hollow debris cloud model was inadequate for predicting the leading and trailing edges of the debris cloud. Particles were all contained within departure angles of less than 20 degrees. There was a cloud of slow, on-axis particles with velocity similar to that predicted by Tate theory. Particle position and size were not correlated.

Modeling was conducted with AUTODYN (SPH) and EPIC, using the mesh-to-particle routine. Both codes predicted similar results; EPIC

results are shown in Fig. 5. In agreement with the data, there is a dense cloud of slow channel fragments on axis. In agreement with the data, almost all particles were less than about 20 mg.
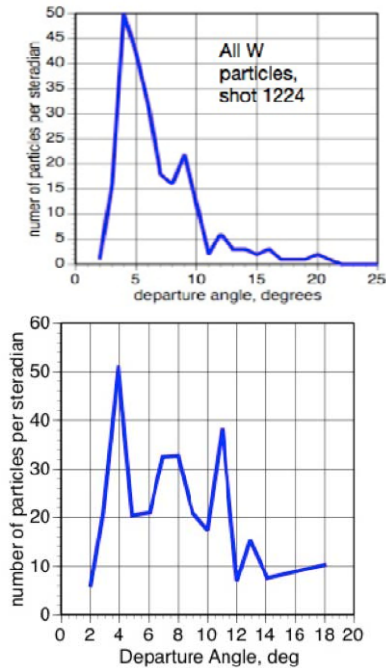

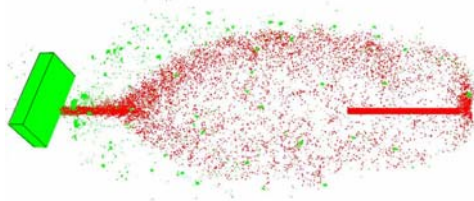**Figure 4.** Flux of particles from shots 1224 (top) and 1225 (bottom).

Figure 5. EPIC simulation of a tungsten rod penetrating steel at 2 km/s.

REFERENCES

1. Saucier, R., Shnidman, R. and Collins III, J., "A stochastic behind-armor debris model," 15th Int. Symp. Ballistics, Jerusalem, Israel, 21–24 May 1995.
2. Tate, A., "Further results in the theory of long rod penetration," J. Mech. Phys. Solids **17**, 141 (1969).
3. Grady, D., "Local Inertial Effects in Dynamic Fragmentation," J. Appl. Phys. **53** pp, 322–325 (1982).
4. Bless, S., and Pedersen, S., "Fragments produced when tungsten penetrates aluminum," Met. Mat. Trans. A **39**, pp 335-339 (2008).
5. Mayseless, M., Sela, N., Stilp, A., and Hohler, V., "Behind the armor debris distribution functions," 13th Int. Symp. Ballistics, Stockholm, Sweden, 1–3 June 1992.
6. www.ctlab.geo.utexas.edu
7. Jordan, B., and Naito, C., "Calculating fragment impact velocity from penetration data," Int. J. Impact Eng. **37**, pp 530–536 (2010).
8. Malick, D., "The calibration of wallboard for the determination of particle speed," available DTIC AD485059, May 1966.
9. Silsby, G., "Penetration of semi-infinite steel targets by tungsten long rods at 1.3 to 4.5 km/s," 8th Int. Symp. Ballistics, Orlando, FL, October 1984.
10. Subramanian, R., and Bless, S., "Reference correlations for tungsten long rods striking semi-infinite steel targets," 19th Int. Symp. Ballistics, Interlaken, Switzerland, 7–11 May 2001.
11. Bless, S., Gee, D., and Pedersen, B., "Yaw degradation of hypervelocity long rods striking space-containing steel targets," Int. J. Impact Eng. **29**, pp 117–126 (2003).